Received: 22 July 2020 | Revised: 19 August 2020 | Accepted: 26 August 2020

DOI: 10.1002/mrc.5092

WILEY

RESEARCH ARTICLE

CRAFT for NMR lipidomics: Targeting lipid metabolism in leucine-supplemented tumor-bearing mice

Hayden Johnson[1] | **Melissa Puppa**[2] | **Marie van der Merwe**[2] | **Aaryani Tipirneni-Sajja**[1]

[1]Department of Biomedical Engineering, The University of Memphis, Memphis, TN, USA

[2]College of Health Sciences, The University of Memphis, Memphis, TN, USA

Correspondence
Aaryani Tipirneni-Sajja, PhD, Department of Biomedical Engineering, The University of Memphis, Memphis, TN 38152, USA.
Email: aaryani.sajja@memphis.edu

Abstract

Lipid profiling by ^{1}H-NMR has gained increasing utility in many fields because of its intrinsically quantitative, nondestructive nature and the ability to differentiate small molecules based on their spectral location. Most nuclear magnetic resonance (NMR) techniques for metabolite quantification use frequency domain analysis that involves many user-dependent steps such as phase and baseline correction and quantification by either manual integration or peak fitting. Recently, Bayesian analysis of time-domain NMR data has been shown to reduce operator bias and increase automation in NMR spectroscopy. In this study, we demonstrate the use of CRAFT (complete reduction to amplitude–frequency table), a Bayesian-based approach to automate processing in NMR-based lipidomics using lipid standards and tissue samples of healthy and tumor-bearing mice supplemented with leucine. Complex mixtures of lipid standards were prepared and examined using CRAFT to validate it against conventional Fourier transform (FT)-NMR and derive a fingerprint to be used for analyzing lipid profiles of serum and liver samples. CRAFT and FT-NMR were comparable in accuracy, with CRAFT achieving higher correlation in quantifying several lipid species. Analysis of the serum lipidome of tumor-bearing mice revealed hyperlipidemia and no signs of hepatic triglyceride accumulation compared with that of the healthy group demonstrating that the tumor-bearing mice were in a state of precachexia. Leucine-supplementation was associated with minimal changes in the lipid profile in both tissues. In conclusion, our study demonstrates that the CRAFT method can accurately identify and quantify lipids in complex lipid mixtures and murine tissue samples and, hence, will increase automation and reproducibility in NMR-based lipidomics.

KEYWORDS

^{1}H, cachexia, CRAFT, leucine, lipid, lipidomics, NMR

1 | INTRODUCTION

Lipids are a large group of organic compounds that form the basis of several major groups of biomolecules such as fatty acids, glycerolipids, phospholipids, and sterols. These lipids have key roles in living systems as energy reservoirs, signaling molecules, protein traffickers, and as the primary constituents of biological membranes. Dysregulation of lipids accompanies a vast number of increasingly common physiological conditions including diabetes, metabolic syndrome, and cancer. Hence, the ability to measure the lipid profile can provide valuable insight into etiology and pathophysiology of diseases.[1–3] Identification and quantification of all lipids in a biological sample are the basis of the steadily growing field of lipidomics, a relatively young '-omics' field that provides phenotypic information complementary to the more upstream fields of proteomics, transcriptomics, and genomics. Lipidomics is a broad discipline with applications in monitoring food quality, disease biomarker discovery, drug safety assessment, nutrition, plant research, and more.[4,5]

Nuclear magnetic resonance (NMR) spectroscopy and mass spectrometry (MS) are the two major analytical techniques used in lipidomics. Although MS has been widely used for lipidomics because of its high sensitivity, NMR is emerging as a potential powerful tool because of several advantages such as it is nondestructive, is intrinsically quantitative, has high analytical reproducibility, and does not need elaborate sample preparation.[3,6] Another important advantage is that the in vitro metabolites detected using NMR, if abundant in the tissue of interest, can be followed noninvasively using high-field clinical MR scanners via in vivo magnetic resonance spectroscopy for noninvasive diagnosis and monitoring of diseases.[7–9] NMR spectroscopy provides a relatively comprehensive method for screening biofluids and even analyzing intact tissue samples. Recently, low-field benchtop NMR spectrometers have been recognized as a cheaper, accessible, and more 'point of care' option for researchers and clinics.[10,11]

^{1}H-NMR spectroscopy is a robust technique used in molecular analysis, capable of distinguishing the major classes of lipids as well as several individual lipid species based on the characteristic spins of the protons that make up these molecules.[1–3] In NMR spectroscopy, the signal is measured as a function of time and is known as the free induction decay (FID). Conventionally, a Fourier transform (FT) is used to convert the FID to the more recognizable frequency domain spectra. The conventional FT-NMR workflow requires preprocessing in the form of apodization and zero filling, as well as phase and baseline correction of the spectra, which may introduce error and interoperator variability in quantification. Quantifying spectra in FT-NMR involves setting integral bounds to determine peak area or otherwise using a peak fitting function to determine peak area. These steps further compound variability between labs and users as integrals are very sensitive to baseline and phasing, whereas peak fitting requires more experience to achieve consistent results.[7,8] Algorithms to characterize parameters of NMR spectra (i.e., frequency, amplitude, line width, and phase) directly in the time domain using Bayesian probability theory have proven effective in the quantitative analysis of complex mixtures.[9,12–15] One of the major benefits of Bayesian time-domain analysis is that the amplitude estimate for a given resonance is essentially independent of its relative phase with respect to the other resonances in the FID. Also, resonances characterized using a Bayesian approach have been shown to provide a better basis for univariate and multivariate statistical analysis, making them ideal for NMR research in metabolomics or lipidomics.[16]

CRAFT (complete reduction to amplitude frequency table) is one such approach that converts a time-domain FID to a frequency–amplitude table in a robust, automated, and time-efficient fashion and has been proven effective in both 1D and 2D NMR.[15–17] In CRAFT, the FID is first digitally filtered and downsampled to several sub-FIDs, and then these sub-FIDs are modeled as sums of decaying sinusoids using Bayesian probability theory.[17] Previously, CRAFT has been validated in purity analysis, untargeted metabolomics, and has even been shown effective in conjunction with data processing using nonuniform sampling.[17,18]

CRAFT analysis can be can performed either on the entire spectra to allow for untargeted analysis or as a specific regional analysis for targeted approach. The untargeted method allows the user to select the spectral width of each segment for the entire spectrum, whereas specific segments are set prior in the targeted method. Each segment is a range of chemical shift values that is treated as an individual sub-FID in CRAFT processing, and the complete set of segments is called a fingerprint. Once the fingerprint is established for a certain cohort, the workflow becomes simplified for targeted analysis. The output from CRAFT analysis is a text file containing all the important spectral information required for quantification such as the frequency of each resonance and amplitude (analogous to peak area in FT-NMR). This automated 'FID to spreadsheet' method has the possibility to improve speed of analysis and lower operator bias in quantification.

In this study, we demonstrate the use of the CRAFT approach to increase automation, reduce operator bias, and improve reproducibility in NMR-based lipidomics

research. The present study uses a targeted approach to create segments in spectral regions by first identifying resonances of interest via lipid standards and using these segments to analyze lipid profiles of biological tissue samples. To the best of our knowledge, CRAFT has yet to be utilized in the context of lipid profiling of biological tissues or in dietary research. The purpose of this study is to validate CRAFT technique for absolute quantification of lipid standards by comparing with volumetric concentrations and conventional FT-NMR analysis and to evaluate the feasibility of CRAFT in quantifying and comparing lipid concentrations in serum and liver samples of healthy and Lewis lung carcinoma (LLC)-implanted mice with leucine supplementation.

2 | MATERIALS AND METHODS

2.1 | Lipid standards

Lipid standards for linoleic acid, cholesterol, cholesteryl oleate, cholesteryl linoleate, palmitic acid, trilinolein, tripalmitin, one gas chromatography lipid standard mixture, and one thin-layer chromatography (TLC) lipid standard mixture were purchased from Nu-Chek Prep. Phosphatidylethanolamine (1,2-dipalmitoyl-sn-glycero-3-phosphoethanolamine) was purchased from TCL America, and phosphatidylcholine (1,2-dioleoyl-sn-glycero-3-phosphocholine) was purchased from Avanti Polar Lipids. The following lipid groups and species were quantified in lipid standards: total triglycerides, total cholesterol, total fatty acids (Total FA), monounsaturated fatty acids (MUFA), polyunsaturated fatty acids (PUFA), linoleic acid, arachidonic acid (ARA), eicosapentaenoic acid (EPA), docosahexaenoic acid (DHA), phosphatidylcholine (PC), and phosphatidylethanolamine (PE). By individually dividing both PUFA and MUFA by the Total FA concentration, the PUFA% and MUFA% were obtained for each mixture. As the ARA and EPA resonances used for identification overlap extensively, these fatty acids are quantified together as ARA + EPA.

NMR samples of all lipid standards, as well as seven lipid mixtures with physiologically relevant concentrations, were prepared by weighing an appropriate amount of lipid standard and solubilizing in 575 μL of deuterated solvent. The composition of these lipid mixtures can be seen in Tables S1–S3. All lipid standards were solubilized in a deuterated three solvent mixture (3SS-d) of chloroform-d, methanol-d, and deuterium oxide (16:7:1–v/v/v) containing 1.18-mM dimethyl sulfone ($DMSO_2$) as an internal quantitative reference and 0.02% (v/v) tetramethylsilane (TMS) as a chemical shift reference. The NMR samples were cooled to 0°C to shift the water signal to ~4.7 ppm, where no major lipid resonances were present.[1] $DMSO_2$ is used for quantification in 3SS-d over the more popular TMS as it is less volatile, and it does not overlap any lipid peaks as it resonates at ~3.0 ppm.[19]

2.2 | Serum and liver samples

Serum and liver samples were collected from tumor-bearing mice undergoing a dietary treatment to improve muscle turnover/protein synthesis.[20] This study involved 20 male C57BL/6 mice, half of which were injected subcutaneously on the flank with $1 * 10^6$ cells of LLC at 9–10 weeks of age. Both groups were further divided with half of each group consuming a regular chow diet (Chow, Chow + LLC), and the other half consumed chow supplemented with 5% leucine (Leu, Leu + LLC).[20] Leucine supplementation has been shown to have many potential beneficial effects on metabolism, often promoting protein synthesis, modulating mitochondrial dysfunction, and accelerating oxidation of fatty acids.[18,21] Mice were euthanized after 4 weeks of supplementation, and livers and serum were harvested and stored at −80°C.

Both serum and hepatic lipids were extracted using a modified version of the Mayatash method of liquid–liquid extraction using methyl tert-butyl ether (MTBE).[21,22] This method has been proven to be at least as efficient at extracting a broad range of lipid classes as the more traditional Bligh and Dyer or Folch methods, which both utilize the carcinogen chloroform as the organic phase. Using MTBE also has the added benefit that the lipid is the top layer, which makes recovery of the lipid layer easier than the above-mentioned traditional methods, which require pipetting past a proteinous matrix layer.[21,22]

For the hepatic lipid extraction, liver tissue was removed from the freezer and ~85 mg was weighed directly in a 2-mL bead mill tube. Cold methanol (MeOH) of ~1.48 mL was added to the weighed tissue sample, and the samples were homogenized for 90 s using a bead mill homogenizer. About 1.31 mL of homogenate (~75 mg of liver tissue) was transferred to a 15-mL centrifuge tube, and 1.7 mL of MTBE was added to each tube and vortexed to mix. After incubating the solution mixture for 1 h at room temperature, 1.57 mL of water was added to induce phase separation. The solution was vortexed to mix, and after an additional 10-min incubation at room temperature, the tube was centrifuged at 2415 × *g* for 10 min. The top (organic/MTBE) layer was removed carefully to a 10-mL beaker, and the bottom (aqueous) layer was re-extracted using 1.5 mL of extraction solvent [MTBE:MeOH:H_2O] (2.6/2.0/2.4–v/v/v). Re-

extraction involved a further 10-min incubation at room temperature and 10-min centrifugation. The top lipid layer was again removed and was pooled with the previously removed lipid fraction before drying under a stream of nitrogen. The dried lipids were resolubilized in 575 μL of 3SS-d before transferring each sample to a 5-mm tube for NMR spectroscopy.

Serum was stored in prealiquoted microcentrifuge tubes. For the serum lipid extraction, 200 μL of serum and 505 μL of MeOH were added to a centrifuge tube and vortexed, followed by adding 656 μL of MTBE. This solution was incubated at room temperature for 1 h before adding 606 μL of deionized water. After a further 10-min incubation at room temperature, the mixture was centrifuged at 2415 × *g* for 10 min. As with the liver samples, the top layer was removed carefully to a 10-mL beaker, and the bottom layer was re-extracted using 1.5 mL of extraction solvent. The top lipid layers were pooled and subsequently dried under a stream of nitrogen. The dried lipids were resolubilized in 575 μL of chloroform-d with 0.03% TMS (v/v) before transferring each sample to a 5-mm tube for NMR spectroscopy. TMS was used as both the quantitative and chemical shift reference in chloroform-d solvent. Serum experiments were performed prior to liver experiments, and the switch from chloroform-d to 3SS-d for liver samples allowed for a shift in the water resonance. Serum ARA + EPA and PE are not quantified because of the chemical shift (∼1.7 ppm overlaps with ARA + EPA) and magnitude of the water resonance, in addition to the lower relative abundance of these lipids in our serum samples.

2.3 | NMR acquisition and spectral processing

A 400-MHz JEOL ECZ NMR spectrometer was used for all spectroscopic measurements. Before acquiring spectra from lipid standards and liver samples, the spectrometer was cooled to 0°C to shift the water resonance. For lipid standards and liver samples, 32 FIDs were recorded with eight dummy scans using a single-pulse proton sequence with presaturation of the water resonance. Preliminary experiments were performed using lipid standards to determine the power of irradiation necessary to attenuate interfering water signal in 3SS-d solution without affecting other resonances of interest. Prior to quantitative spectra acquisition, a four-scan single-pulse proton sequence was collected to check shimming and locate the chemical shift of the water resonance (∼4.7 ppm). Serum measurements were taken at ambient temperature without presaturation of the water resonance. A larger number of scans (512 FIDs) were obtained for serum measurements because of the lower signal-to-noise ratio obtained without water presaturation. The following parameters were the same for all FIDs recorded—pulse angle, 45°; relaxation delay, 4 s; repetition time, 12.75 s; and FID acquisition time, 8.75 s.

The spectral processing for all samples was performed in JEOL Delta v5.3 software using CRAFT. In addition, lipid standards were also processed with Delta v5.3 software using conventional FT-NMR for validation. For FT-NMR analysis, each FID was zero-filled two times and apodised with a 0.3-Hz line broadening function prior to Fourier transformation. Spectra were then machine-phased (a built-in auto-phasing function), and the baseline was corrected using an Akima algorithm. Peak areas of identified lipids were determined using a built-in deconvolution function. Peaks were fit to a mixed, Voigt distribution.

Fingerprint for lipids in 3SS-d and chloroform-d was first created using lipid standards. A representative workflow for using CRAFT in NMR-lipidomics research is shown in Figure 1. The FID is first opened in the CRAFT tool, and the appropriate fingerprint is selected. Prior to FID analysis, it is important to ensure the region of interest threshold and peak result threshold are set low enough to detect all necessary peaks. Both thresholds were set to 0.05% for all samples. For post-acquisition solvent suppression, the 'H_2O' option under 'HD CRAFT' was selected for serum samples, whereas 'Methanol OH Only' option was selected for lipid standards and liver samples as water was already suppressed. Each spectrum was assessed visually before submission to ensure all peaks were still in the correct segment, given that relative changes in metabolite levels have the potential to shift peaks slightly. The TMS resonance was not aligned to 0 ppm for fingerprint analysis in CRAFT. Upon processing of the FID signal, amplitude–frequency table is generated as the output and the CRAFT amplitudes are used to calculate lipid concentrations.

Lipid concentrations were determined using the following equation: $\boldsymbol{M_x = A_x} * \left(\frac{\boldsymbol{M_{ref}}}{\boldsymbol{A_{ref}}}\right) * \left(\frac{\boldsymbol{N_{ref}}}{\boldsymbol{N_x}}\right)$, where M_x is the analyte concentration, M_{ref} is the reference concentration, A_x is the analyte peak area or amplitude, A_{ref} is the reference peak area or amplitude, N_x is the number of protons contributing to the analyte peak, and N_{ref} is the number of protons contributing to the reference peak.[1]

2.4 | Statistical analysis

For lipid standards, linear regression analysis was performed to compare NMR calculated concentrations obtained from CRAFT and FT-NMR to volumetric

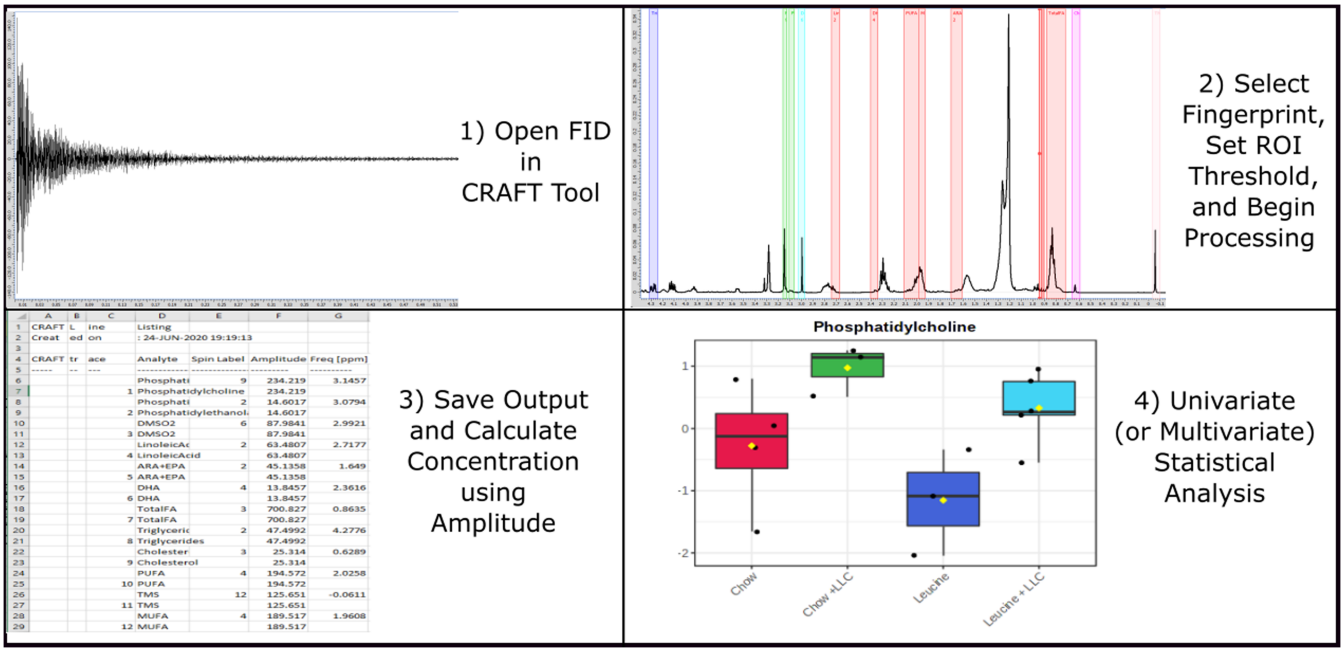

FIGURE 1 CRAFT workflow for NMR-based lipidomics research. The FID is first opened in the CRAFT tool, an appropriate fingerprint is selected for targeted analysis, and an ROI threshold is set for calculating the amplitude–frequency table. The amplitudes are then converted into lipid concentrations, and statistical analysis is performed to reveal differences and interactions between variables and subgroups

concentrations. The lipid data obtained from serum and liver samples were autoscaled and normalized through logarithmic data transformation using MetaboAnalyst (https://www.metaboanalyst.ca), an online tool for comprehensive analysis of metabolomics data.[23,24] Two-way analysis of variance (ANOVA) was used to determine the main effects and/or interactions between all four groups, and *t*-test was used to determine statistical differences between subgroups using MetaboAnalyst. Statistical significance for all tests was defined as a p value lower than 0.05.

3 | RESULTS AND DISCUSSION

The fingerprint of the resonances used in lipid quantification was created by analyzing lipid standards in 3SS-d and can be found in Table 1. As serum experiments were performed in chloroform-d rather than in 3SS-d, a slightly modified fingerprint was used and is shown in Table 2. Examination of spectra of individual lipid standards as well as complex lipid mixtures confirmed that most of the quantified lipids did not significantly overlap any other resonances. The only exceptions were those for MUFA at ~2.0 ppm and Total FA at ~0.88 ppm whose ^{1}H NMR signals both directly overlap cholesterol proton resonances. The unambiguous total cholesterol peak at ~0.695 ppm was used to determine the contribution of the cholesterol protons in each spectrum, and the magnitude of overlap was subtracted from the MUFA and Total FA amplitudes before concentration calculations.

TABLE 1 CRAFT segments used for measurements of lipid metabolites in 3SS-d solvent determined from lipid standards

Analyte	Segment (ppm)
TMS	(−0.044)–(0.018)
TC	0.645–0.686
Total FA	0.759–0.923
ARA + EPA	1.614–1.707
MUFA	1.955–2.020
PUFA	2.017–2.148
DHA	2.346–2.403
Linoleic acid	2.714–2.764
$DMSO_2$	2.972–3.023
PE	3.061–3.107
PC	3.310–3.348
TG	4.244–4.305

Abbreviations: ARA, arachidonic acid; CRAFT, complete reduction to amplitude–frequency table; DHA, docosahexaenoic acid; $DMSO_2$, dimethyl sulfone; EPA, eicosapentaenoic acid; MUFA, monounsaturated fatty acids; PC, phosphatidylcholine; PE, phosphatidylethanolamine; PUFA, polyunsaturated fatty acids; TC, total cholesterol; TG, total triglycerides; TMS, tetramethylsilane; Total FA, total fatty acids.

TABLE 2 CRAFT segments used for measurements of lipid metabolites in chloroform-d solvent for serum samples

Analyte	Segment (ppm)
TMS	(−0.044)–(0.018)
TC	0.645–0.686
Total FA	0.759–0.923
ARA + EPA	1.614–1.707
MUFA	1.955–2.020
PUFA	2.017–2.148
DHA	2.346–2.403
Linoleic acid	2.714–2.764
$DMSO_2$	2.972–3.023

Abbreviations: ARA, arachidonic acid; CRAFT, complete reduction to amplitude–frequency table; DHA, docosahexaenoic acid; $DMSO_2$, dimethyl sulfone; EPA, eicosapentaenoic acid; MUFA, monounsaturated fatty acids; PUFA, polyunsaturated fatty acids; TC, total cholesterol; TMS, tetramethylsilane; Total FA, total fatty acids.

The results from the seven lipid standard mixtures (Table 3; scatter plots in supplement) showed high correlations ($R^2 \geq 0.86$) between concentrations estimated from CRAFT and volumetric concentrations and demonstrated high accuracy with slopes close to 1 (0.9–1.2). The conventional FT-NMR-derived concentrations also showed similar results except for MUFA, DHA, MUFA%, and PUFA%. The better results achieved using CRAFT to quantify these resonances and percentages are likely due to the limited number of user-dependent steps compared with FT-NMR and the overall consistency of the CRAFT method. These results show that CRAFT can be at least as accurate as the almost ubiquitous FT-NMR in lipid profiling of complex mixtures. More importantly, CRAFT successfully increased automation and speed in the data processing portion of our NMR lipidomics workflow, with an average ∼4–5 min from FID processing to the generation of the frequency–amplitude table.

Hepatic and serum lipid concentrations determined from CRAFT-derived amplitudes for healthy and LLC groups on different diets are shown in Figures 2 and 3. Two-way ANOVA revealed no main effects based on diet in either tissue. Tumor inoculation was associated with increased serum lipid levels, with main effects noted for triglycerides ($p = 0.008$), PUFA ($p = 0.015$), DHA ($p = 0.012$), and PC ($p = 0.006$). Furthermore, *t*-tests revealed increased serum PC in Leu + LLC mice versus Leu mice ($p = 0.025$), as well as increased triglycerides ($p = 0.002$) and linoleic acid ($p = 0.040$) in Chow + LLC compared with Chow. By contrast, hepatic lipids tended to decrease with LLC inoculation, with main effects noted for total FA ($p = 0.013$), MUFA ($p = 0.004$), and PUFA ($p = 0.007$). Leucine supplementation in LLC mice showed statistically significant decreases in hepatic PUFA ($p = 0.021$), total FA ($p = 0.035$), and triglycerides ($p = 0.023$) compared with their healthy counterparts.

Several results from our NMR analysis in murine samples are consistent with the aberrant lipid metabolism expected at some point in cancer-associated cachexia. Cachexia is a wasting syndrome often characterized by a marked decrease in skeletal muscle and fat reserves, and it is a leading cause of death in many cancers.[25] Further, cachexia is a complex condition that increases in severity over time as host energy metabolism becomes increasingly altered. Blood from cachectic patients typically shows high levels of lipids such as fatty acids and triglycerides.[25] Increased levels of phospholipids and choline-containing lipids have also been linked to the metastasis of cancer cells in past lipidomic studies.[26,27] Researchers examining the plasma metabolome of mice implanted with LLC using UPLC-QTOF/MS noted glycerophospholipid metabolism to be the most significantly disturbed metabolic pathway in their study.[28] Our serum samples expressed similar dyslipidemias in tumor-bearing mice evidenced by increased levels of triglycerides, PUFA, and PC compared with that in healthy mice. Previous mouse models have shown that changes in lipid metabolism precede skeletal muscle wasting in cachexia induced by LLC.[29] The onset of steatosis is associated with cachexia, but the LLC mice in this study did not show accumulation of hepatic triglycerides. As the cachectic arc is a complex, progressive disorder of metabolism, it is possible that molecular changes have occurred to increase serum triglycerides to supply nutrients for the tumor that precede steatosis in LLC inoculated mice. The lipid profiles observed in our mice appear consistent with a diagnosis of precachexia, the early cachectic stage characterized by metabolic dysfunction without loss of lean body mass. Results from this study are consistent with the conclusion reached by investigators utilizing tissues from the same mice as the present study and examining protein expression and tissue mass.[20]

According to Abbondante et al., the serum metabolome is more sensitive to nutritional changes than the liver.[30] Our results also support serum as being more sensitive to nutritional alterations; measured serum lipids demonstrated a larger fold change than hepatic lipids with lower *p* values. We expect that extending the study past 28 days may have induced more marked changes in hepatic lipid concentrations; however, this needs future investigation.

Leucine supplementation has previously been shown to result in triglyceride accumulation in hepatic cells, and

TABLE 3 Results from linear regression analysis (slope, R^2, and p values) showing associations between true lipid concentrations and concentrations determined by NMR spectroscopy

	Quantified using CRAFT			Quantified using FT-NMR		
Lipid Species	**Slope**	**R^2**	**p-value**	**Slope**	**R^2**	**p-value**
Total Cholesterol	0.8	0.99	7.5E-07	1.1	>0.99	1.3E-06
Total Triglycerides	0.8	0.99	2.5E-06	1.1	0.99	8.2E-07
Linoleic Acid	1.1	>0.99	1.1E-08	1.0	>0.99	1.0E-05
MUFA	0.7	0.86	2.5E-03	0.3	0.48	8.5E-02
PUFA	1.0	>0.99	5.3E-08	1.0	>0.99	1.2E-07
Total FA	0.9	>0.99	1.1E-07	1.0	>0.99	1.4E-08
MUFA%	0.9	0.97	3.6E-05	0.6	0.88	1.8E-03
PUFA%	1.0	0.99	5.2E-06	0.7	0.98	2.4E-05
DHA	0.8	>0.99	3.7E-02	1.7	0.99	5.2E-02
ARA	0.9	>0.99	2.0E-02	1.2	0.98	9.9E-02
PC	1.1	>0.99	9.0E-03	1.0	>0.99	9.0E-03
PE	1.0	>0.99	3.2E-02	1.2	0.99	5.5E-02

Abbreviations: ARA, arachidonic acid; CRAFT, complete reduction to amplitude–frequency table; DHA, docosahexaenoic acid; $DMSO_2$, dimethyl sulfone; EPA, eicosapentaenoic acid; FT-NMR, Fourier transform nuclear magnetic resonance; MUFA, monounsaturated fatty acids; NMR, nuclear magnetic resonance; PC, phosphatidylcholine; PE, phosphatidylethanolamine; PUFA, polyunsaturated fatty acids; TC, total cholesterol; TG, total triglycerides; TMS, tetramethylsilane; Total FA, total fatty acids.

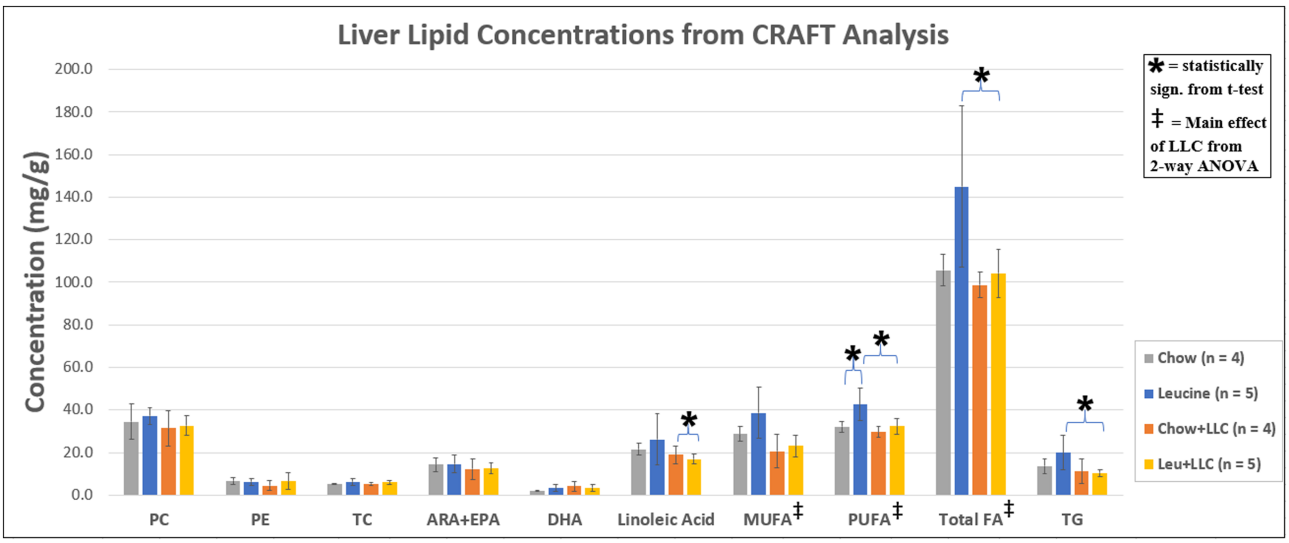

FIGURE 2 Hepatic lipid profile and statistical differences between healthy and LLC mice on different diets (chow, leu) noted from t-tests and two-way ANOVA ($p < 0.05$). With LLC inoculation, hepatic lipids tended to decrease with the main effects noted for total FA, MUFA, and PUFA. With leucine supplementation, LLC mice showed significant decreases in PUFA, total FA, and triglycerides compared with the healthy mice

in our study, the leu group expressed higher triglyceride levels than the chow group.[31] The leucine-fed mice implanted with LLC did not show a similar increase in hepatic triglycerides.[32] Other studies note increased triglycerides in healthy mice supplemented with leucine and other branched-chain amino acids, and reduced hepatic triglycerides in supplemented mice subject to a metabolic challenge such as genetically obese db/db mice or mice fed a high-fat diet.[33,34] The cause for this apparent inconsistency, and the fact that all main effects (ANOVA) were due to LLC, may be due to the molecular machinery that participates in general energy and lipid metabolism being altered during the progression of cachexia.[37]

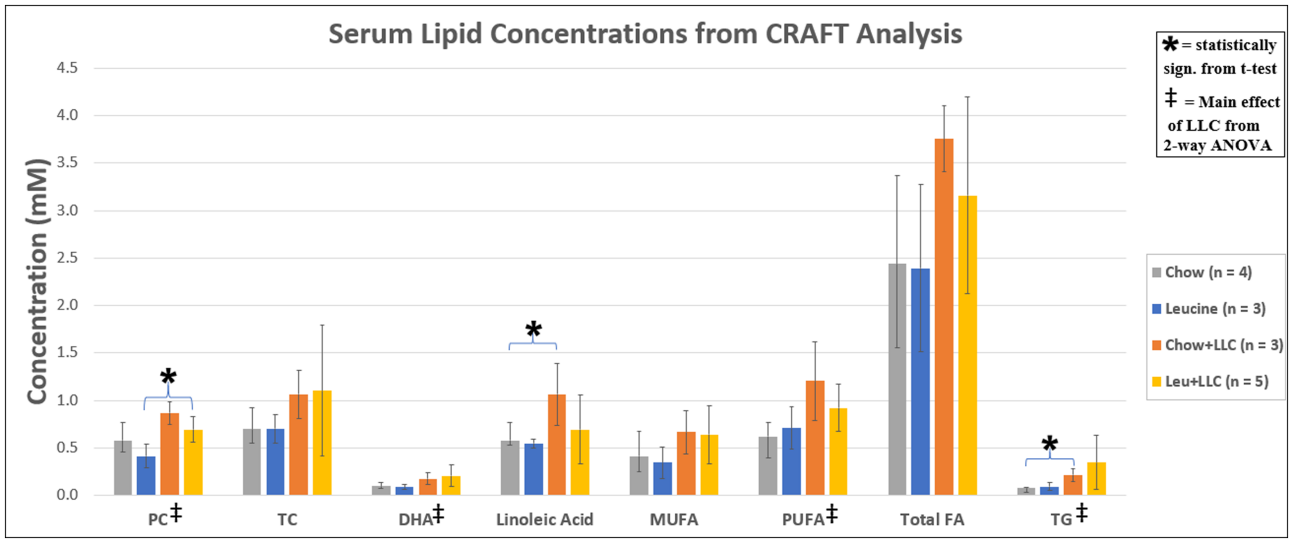

FIGURE 3 Serum lipid profile and statistical differences between healthy and LLC mice on different diets (chow, leu) noted from *t*-tests and two-way ANOVA ($p < 0.05$). LLC inoculation demonstrated serum hyperlipidemia with main effects noted for PC, DHA, PUFA, and TG. LLC inoculation was associated with increased linoleic acid and TG in chow-fed mice and increased PC in leucine-supplemented mice

It should be noted that reliable absolute quantification in NMR requires sufficient repetition time between pulses to allow more complete signal recovery, with five times the longest T_1 value in solution being the recommended time between pulses. T_1 relaxation times for resonances relevant to this study were calculated by performing inversion recovery experiments with a 90° pulse angle in lipid standard mixtures, and the longest T_1 relaxation times determined were for the quantitative reference peaks (4.27 s for TMS in chloroform-d at ambient temperature (~21°C) and 2.53 s for $DMSO_2$ in 3SS-d at 0°C). The repetition time used in our study was sufficiently long for all lipid resonances to relax in both scenarios, as well as for the $DMSO_2$ resonance in 3SS-d. The longer T_1 relaxation time of TMS in chloroform-d solution has the potential to introduce error in absolute quantification of lipids in serum samples. However, several factors of the study ensure these errors are systematic in nature and do not significantly affect our comparative analysis—primarily that an internal quantitative reference was used, parameters are consistent throughout the dataset, and a smaller pulse angle (45°) was utilized than in the inversion recovery experiment.

There are some limitations in this study. The current study is limited by sample size and in the physical size of the mice, as some of the serum samples that were <200 μL were not sufficient for NMR quantification and, hence, were not used in this study. Utilizing two different solvents for liver and serum samples led to slightly differing CRAFT fingerprints and NMR acquisition parameters; however, we do not believe that these changes could significantly affect the results of this study. As this study was performed in one mouse model bearing a specific tumor, the lipid profile results may not translate directly to other cancers or organisms.

4 | CONCLUSION

Our work demonstrates that CRAFT offers an accurate and automated method to identify and quantify lipids in complex mixtures compared with the almost ubiquitous conventional FT-NMR approach. NMR analysis of murine tissues confirmed that serum was more responsive to metabolic challenge than the liver, with increased serum lipid levels in tumor-bearing mice indicative of cancer progression and precachexia. Leucine supplementation in both healthy and tumor-bearing groups was only associated with minimal changes in the lipid profile in both serum and liver tissues. In summary, this study demonstrates the proof of concept that CRAFT analysis can be used to increase the automation and reproducibility in NMR-based lipidomics.

ACKNOWLEDGEMENTS

The authors wish to acknowledge Dr. Truc Chi Pham from the Chemistry Department at the University of Memphis for instruction with the NMR spectrometer and Dr. Erno Lindner from the Department of Biomedical Engineering for opening his labs for our work as well as continued guidance.

PEER REVIEW

The peer review history for this article is available at https://publons.com/publon/10.1002/mrc.5092.

ORCID

Hayden Johnson https://orcid.org/0000-0001-9945-195X
Melissa Puppa https://orcid.org/0000-0003-3826-0003
Marie van der Merwe https://orcid.org/0000-0001-5683-4790
Aaryani Tipirneni-Sajja https://orcid.org/0000-0002-3246-8711

REFERENCES

[1] R. Barrilero, M. Gil, N. Amigó, C. B. Dias, L. G. Wood, M. L. Garg, J. Ribalta, M. Heras, M. Vinaixa, X. Correig, *Anal. Chem.* **2018**, *90*, 2031. https://doi.org/10.1021/acs.analchem.7b04148
[2] A. Amiel, M. Tremblay-Franco, R. Gautier, S. Ducheix, A. Montagner, A. Polizzi, L. Debrauwer, H. Guillou, J. Bertrand-Michel, C. Canlet, *Metabolites* **2019**, *10*, 9. https://doi.org/10.3390/metabo10010009
[3] E. Alexandri, R. Ahmed, H. Siddiqui, M. Choudhary, C. Tsiafoulis, I. Gerothanassis, *Molecules* **2017**, *22*, 1663. https://doi.org/10.3390/molecules22101663
[4] J. Marchand, E. Martineau, Y. Guitton, B. Le Bizec, G. Dervilly-Pinel, P. Giraudeau, *Metabolomics* **2018**, *14*. https://doi.org/10.1007/s11306-018-1360-x
[5] Y.-Y. Zhao, S.-P. Wu, S. Liu, Y. Zhang, R.-C. Lin, *Chem. Biol. Interact.* **2014**, *220*, 181. https://doi.org/10.1016/j.cbi.2014.06.029
[6] J. Li, T. Vosegaard, Z. Guo, *Prog. Lipid Res.* **2017**, *68*, 37. https://doi.org/10.1016/j.plipres.2017.09.003
[7] T. Schoenberger, *Guideline For qNMR Analysis*. **2020**. https://enfsi.eu/wp-content/uploads/2017/06/qNMR-Guideline_version001.pdf
[8] S. K. Bharti, R. Roy, *TrAC Trends Anal. Chem.* **2012**, *35*, 5. https://doi.org/10.1016/j.trac.2012.02.007
[9] G. L. Bretthorst, *J. Magn. Reson. (1969)* **1990**, *88*, 533. https://doi.org/10.1016/0022-2364(90)90287-j
[10] B. C. Percival, M. Grootveld, M. Gibson, Y. Osman, M. Molinari, F. Jafari, T. Sahota, M. Martin, F. Casanova, M. L. Mather, M. Edgar, J. Masania, P. B. Wilson, *High. Throughput* **2018**, *8*, 2.
[11] J. Leenders, M. Grootveld, B. Percival, M. Gibson, F. Casanova, P. B. Wilson, *Metabolites* **2020**, *10*, 155.
[12] G. L. Bretthorst, *J. Magn. Reson. (1969)* **1990**, *88*, 552.
[13] G. L. Bretthorst, *J. Magn. Reson. (1969)* **1990**, *88*, 571.
[14] G. L. Bretthorst, *J. Magn. Reson. (1969)* **1991**, *93*, 369. https://doi.org/10.1016/0022-2364(91)90013-j
[15] G. L. Bretthorst, *J. Magn. Reson. (1969)* **1992**, *98*, 501. https://doi.org/10.1016/0022-2364(92)90004-q
[16] D. V. Rubtsov, C. Waterman, R. A. Currie, C. Waterfield, J. D. Salazar, J. Wright, J. L. Griffin, *Anal. Chem.* **2010**, *82*, 4479. https://doi.org/10.1021/ac100344m
[17] K. Krishnamurthy, N. Hari, *Magn. Reson. Chem.* **2018**, *56*, 535. https://doi.org/10.1002/mrc.4664
[18] K. Krishnamurthy, *Magn. Reson. Chem.* **2013**, *51*, 821. https://doi.org/10.1002/mrc.4022
[19] E. Martineau, J.-N. Dumez, P. Giraudeau, *Magn. Reson. Chem.* **2020**, *58*, 390. https://doi.org/10.1002/mrc.4899
[20] H. W. Lee, E. Baker, K. M. Lee, A. M. Persinger, W. Hawkins, M. Puppa, *Appl. Physiol. Nutr. Metab.* **2019**, *44*, 997. https://doi.org/10.1139/apnm-2018-0765
[21] J. Sostare, R. Di Guida, J. Kirwan, K. Chalal, E. Palmer, W. B. Dunn, M. R. Viant, *Anal. Chim. Acta* **2018**, *1037*, 301. https://doi.org/10.1016/j.aca.2018.03.019
[22] V. Matyash, G. Liebisch, T. V. Kurzchalia, A. Shevchenko, D. Schwudke, *J. Lipid Res.* **2008**, *49*, 1137. https://doi.org/10.1194/jlr.d700041-jlr200
[23] J. Chong, D. S. Wishart, J. Xia, *Curr. Protoc. Bioinformatics* **2019**, *68*. https://doi.org/10.1002/cpbi.86
[24] J. Xia, I. V. Sinelnikov, D. S. Wishart, *Bioinformatics* **2011**, *27*, 2455. https://doi.org/10.1093/bioinformatics/btr392
[25] P. Saavedra-García, K. Nichols, Z. Mahmud, L. Y.-N. Fan, E. W.-F. Lam, *Mol. Cell. Endocrinol.* **2018**, *462*, 82. https://doi.org/10.1016/j.mce.2017.01.012
[26] F. Yan, H. Zhao, Y. Zeng, *Clin. Transl. Med.* **2018**, *7*. https://doi.org/10.1186/s40169-018-0199-0
[27] E. Currie, A. Schulze, R. Zechner, T. C. Walther, R. V. Farese, *Cell Metab.* **2013**, *18*, 153. https://doi.org/10.1016/j.cmet.2013.05.017
[28] H. Wu, Y. Chen, Z. Li, X. Liu, *R. Soc. Open Sci.* **2018**, *5*, 181143. https://doi.org/10.1098/rsos.181143
[29] P. E. Porporato, *Oncogene* **2016**, *5*, e200. https://doi.org/10.1038/oncsis.2016.3
[30] S. Abbondante, K. L. Eckel-Mahan, N. J. Ceglia, P. Baldi, P. Sassone-Corsi, *J. Biol. Chem.* **2016**, *291*, 2812. https://doi.org/10.1074/jbc.m115.681130
[31] M. D. Neinast, C. Jang, S. Hui, D. S. Murashige, Q. Chu, R. J. Morscher, X. Li, L. Zhan, E. White, T. G. Anthony, J. D. Rabinowitz, Z. Arany, *Cell Metab.* **2019**, *29*, 417. https://doi.org/10.1016/j.cmet.2018.10.013
[32] X. Han, S. H. Raun, M. Carlsson, K. A. Sjøberg, C. Henriquez-Olguín, M. Ali, A. Lundsgaard, A. M. Fritzen, L. L. V. Møller, Z. Li, J. Li, T. E. Jensen, B. Kiens, L. Sylow, *Metabolism* **2020**, *105*, 154169. https://doi.org/10.1016/j.metabol.2020.154169
[33] Y. Zhang, K. Guo, R. E. LeBlanc, D. Loh, G. J. Schwartz, Y.-H. Yu, *Diabetes* **2007**, *56*, 1647. https://doi.org/10.2337/db07-0123
[34] I. Tikhanovich, J. Cox, S. A. Weinman, *J. Gastroenterol. Hepatol.* **2013**, *28*, 125. https://doi.org/10.1111/jgh.12021

SUPPORTING INFORMATION

Additional supporting information may be found online in the Supporting Information section at the end of this article.

How to cite this article: Johnson H, Puppa M, van der Merwe M, Tipirneni-Sajja A. CRAFT for NMR lipidomics: Targeting lipid metabolism in leucine-supplemented tumor-bearing mice. *Magn Reson Chem*. 2020;1–9. https://doi.org/10.1002/mrc.5092